ORIGINAL ARTICLE

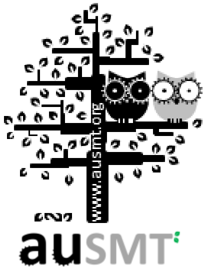

A Planar Laser Diffraction Encoder in Littrow Configuration for 2D Nanometric Positioning

Kuang-Chao Fan, Bor-Cheng Lee, and Yi-Cheng Chung*
Department of Mechanical Engeering, National Taiwan University, Taiwan
(**Received** 24 November 2010; **Accepted** 13 July 2011; **Published on line** 1 December 2011)
*Corresponding author: b94502140@ntu.edu.tw
DOI: 10.5875/ausmt.v1i2.53

Abstract: This paper presents a novel design of a planar encoder based on the principle of diffractive interferometry. The system is capable of measuring the two-dimensional displacement of the planar grating of any size. It adopts a specially designed optical path that can increase the alignment tolerance between the optical head and the grating. Given the merits of its simple optical configuration and compact size, it can effectively reduce the environmental disturbance and allow higher stability. The signal processing circuit and waveform subdivision software were also developed to effectively compensate for the waveform errors and count the position to 1nm resolution. Experimental results showed that even in the normal laboratory environment the standard deviation of measured values can be controlled to within 15 nm for a long stroke up to 25 mm on both axes.

Keywords: Planar encoder; Diffractive interferometer; Planar gratings; Waveform errors

Introduction

Nowadays, the development of many nano-scale manufacturing and measuring systems relies on the nanometric positioning. However, instruments with long measuring distance and nano-scale resolution, such as laser interferometers and laser Doppler displacement systems, are bulky, expensive and sensitive to the atmospheric disturbance because the basic length unit used is the wavelength. A linear encoder, based on the principle of Morié fringes, is widely used in the industry for long-stroke measurement, but it has limited resolution and accuracy due to its large grating pitch. Thus, to develop a displacement sensor that is compact, low cost, high resolution and noise immune is becoming more indispensable.

In recent years, many linear displacement sensors with nano-scale resolution have been developed [1-3]. However, two dimensional sensors of this kind are relatively complicated and rare. Traditional 2D displacement sensors are usually stacked up by a pair of 1D sensors in cross configuration. The alignment tolerance of the sensor head to the scale is critical and subjected to metrology errors. Therefore, developing a high resolution and high accuracy 2D displacement sensor which possesses high alignment tolerance is urgently needed.

Toward this end, Mitutoyo Co. [4] used three linear gratings in each dimension to form a planar encoder that was considered to be a complicated design. Lee [5] developed a special conjugate optical design to achieve nano-scale resolution. Gao [6] proposed a surface encoder which is composed of a slope-sensor and a grid and has the ability to measure multi-DOF. Kao [7] proposed a double diffraction optical design using conjugate optics to achieve nano-resolution. Gao [8] developed a novel three-axis displacement sensor composed of Michelson interferometry and grating interferometry by using two planar gratings. Akihide [9] proposed a two-DOF linear encoder that could measure the X-directional position and the Z-directional

Copyright © 2011 International Journal of Automation and Smart Technology

straightness simultaneously. In regard to these attempts, it is noted that although the principles are sound in most of the above-mentioned research, they could not successfully demonstrate the capability of long stroke and nano accuracy through experiments.

This paper presents a planar encoder using grating interferometry to obtain 2D displacement measurements to nanometer resolution. The main purpose of optical configuration design is to obtain high resolution and reduce the alignment errors. This novel optical design has simple optical configuration and high alignment tolerance. In order to compensate for the inevitable geometric errors of the moving stage, hardware and software signal processing are carried out. Experiments demonstrate the capability of this planar encoder in long stroke and high accuracy measurement.

Design Principle

Measurement Principle

The proposed planar encoder, which is named planar diffraction grating interferometer (PDGI), is composed of an optical read head and a planar grid. It is a grating interferometer which obtains 2-D displacement by using the Doppler Effect.

The optical system of PDGI is designed in Littrow configuration, where the incident laser beam is diffracted back through the same optical path. That is, the laser beam is emitted to the grating at the first order diffraction angle, as shown in Figure 1. The incident angle is set according to the grating equation:

$$\theta_{Littrow} = \sin^{-1}\frac{m\lambda}{2d} \qquad (1)$$

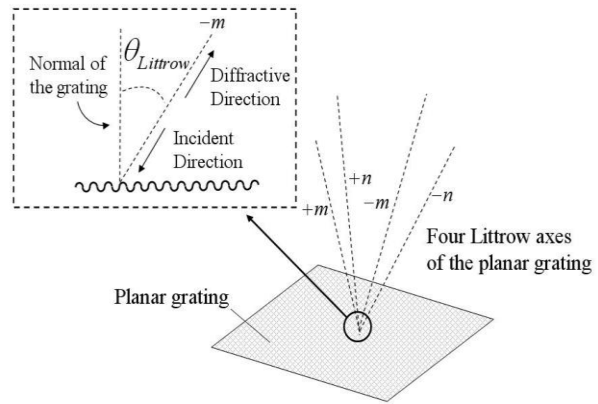

Figure 1. Littrow configuration of the planar grating.

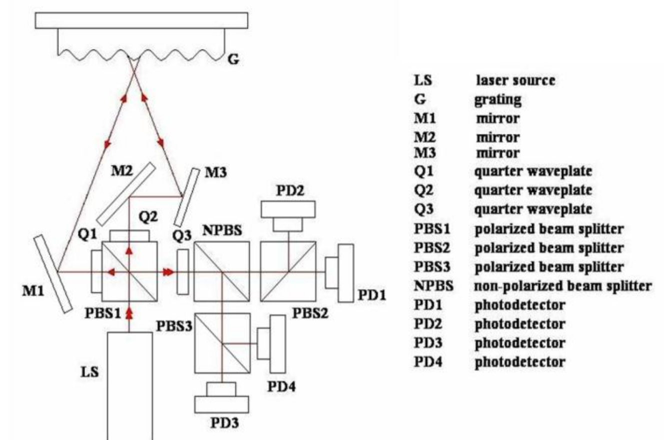

Figure 2. Principle of the LDGI.

where λ is the wavelength of the incident beam, m denotes the diffraction order and d is the grating pitch. The merit of Littrow configuration is that it can enhance the encoder's geometric tolerance against mechanical wobble of the grating.

The principle of PDGI is the combination of two linear diffraction grating interferometers (LDGI) arranged in orthogonal directions. Figure 2 shows the configuration of the LDGI system. The laser diode emits a linearly polarized beam that is split by a polarizing beam splitter (PBS) with equal intensity. The P-polarized beam propagates along the right side of the optical path. The quarter waveplate (Q2) converts the P-polarized beam into a right-circularly polarized beam. Simultaneously, the S-polarized beam propagates along the left side of the optical path, and then is converted into a left-circularly polarized beam after Q1. These two circularly polarized light beams are reflected by mirrors (M1–M3) and diffracted by the grating. Designed with Littrow configuration, the two incident angles equal to the grating's ±1th order diffraction angles, each input beam will be diffracted back through the same path to the corresponding mirror. The left-arm beam is changed to a P-polarized beam after it transmits through Q1.

Kuang-Chao Fan received the B.S. degree from National Taiwan University in 1972, M.S. degree from the State University of New York at Buffalo in USA in 1976, and Ph.D. degree from University of Manchester Institute of Science and Technology in UK in 1984, all in mechanical engineering. He is the lifetime distinguished professor and Zhong-Juo Zhang Chair in the Department of Mechanical Engineering of National Taiwan University (NTU). In NTU, he was the Chairman of Institute of Industrial Engineering, the Director of Tjing Ling Industrial Research Institute, and the Associate Dean of Engineering College. He served as the Chairman of Chinese Institute of Automation Technology (CIAE), the Chairman of SME Taipei Chapter, and the Board member of Chinese Society of Mechanical Engineers (CSME). He is the elected Fellow of SME, CSME and CIAE. He is also the Changjian Scholar at Hefei University of Technology in China. His research interests include manufacturing metrology, optical measurements, micro/nano-measurements, and machine tool metrology. He has published more than 100 journal papers and 200 conference papers.

Bor-Cheng Lee received the M.S. degree in mechanical engineering from National Taiwan University in 2010. His research interests include optical measurements and laser encoder.

Yi-Cheng Chung received the M.S. degree in mechanical engineering from National Taiwan University in 2011. His research interests include displacement transducer and angle sensor.

Copyright © 2011 International Journal of Automation and Smart Technology

Similarly, the right-arm beam is changed to a S-polarized beam after it transmits through Q2. After passing through the quarter waveplate Q3, these two beams are retarded to the left-circularly polarized and right-circularly polarized beams, respectively.

According to the Doppler effect, a frequency shift of the first order diffraction beams will occur as soon as the grating moves. The actual frequencies of the two diffraction beams in LDGI can be derived as

$$f_{+1} = f_0 + \frac{v}{d},\ f_{-1} = f_0 - \frac{v}{d} \tag{2}$$

where f_0 is the frequency of incident beam, f_{+1} is the frequency of the +1st-order diffraction beam, f_{-1} is the frequency of the -1st-order diffraction beam, and v is the velocity of the grating.

Thus, the interference fringes created in the photodetectors (PDs) also shift due to the beating frequency:

$$\Delta f = f_{+1} - f_{-1} = \frac{2v}{d},\ \Delta\omega = 2\pi\Delta f = \frac{4\pi v}{d} \tag{3}$$

Therefore, the electric fields of the two beams propagating from Q3 are:

$$\begin{aligned} \vec{E_L} &= a \cdot \exp\left[i\left(\omega - \frac{\Delta\omega}{2}t\right)\right]\begin{bmatrix}1\\ i\end{bmatrix} \\ \vec{E_R} &= a \cdot \exp\left[i\left(\omega + \frac{\Delta\omega}{2}t\right)\right]\begin{bmatrix}1\\ -i\end{bmatrix} \end{aligned} \tag{4}$$

where a is the amplitude of the electric field, and the last 2D vectors stand for the Jones vector of the two beams, respectively. Table 1 lists the mathematical expression of Jones vectors of corresponding optics.

Table 1. Jones vector (matrix) of some polarization or optics.

Polarization or optics	Mathematical expression
Right Circular Polarization	$\frac{\sqrt{2}}{2}\begin{bmatrix}1\\ -i\end{bmatrix}$
Left Circular Polarization	$\frac{\sqrt{2}}{2}\begin{bmatrix}1\\ i\end{bmatrix}$
PBS, horizontally installed	Through: $\begin{bmatrix}1 & 0\\ 0 & 0\end{bmatrix}$ Reflection: $\begin{bmatrix}0 & 0\\ 0 & 1\end{bmatrix}$
PBS, with 45° rotation of fast axis	Through: $\frac{1}{2}\begin{bmatrix}1 & 1\\ 1 & 1\end{bmatrix}$ Reflection: $\frac{1}{2}\begin{bmatrix}1 & -1\\ -1 & 1\end{bmatrix}$

The non-polarized beam splitter (NPBS) divides both the right-circularly and the left-circularly polarized beam into two split beams of equal intensity. These four beams will be divided into 0-90-180-270 degrees of polarization by PBS2 and PBS3 (set fast axis to 45 degrees). The electric fields of the beams on the four PDs are:

$$\begin{aligned} \overrightarrow{E_{PD1}} &= \begin{bmatrix}1 & 0\\ 0 & 0\end{bmatrix}\left(\vec{E_L} + \vec{E_R}\right) \\ &= \begin{bmatrix}1\\ 0\end{bmatrix} 2a\exp(i\omega t)\cos(\Delta\omega t) \\ \overrightarrow{E_{PD2}} &= \begin{bmatrix}0 & 0\\ 0 & 1\end{bmatrix}\left(\vec{E_L} + \vec{E_R}\right) \\ &= \begin{bmatrix}0\\ 1\end{bmatrix} 2a\exp(i\omega t)\sin(\Delta\omega t) \\ \overrightarrow{E_{PD3}} &= \frac{1}{2}\begin{bmatrix}1 & -1\\ -1 & 1\end{bmatrix}\left(\vec{E_L} + \vec{E_R}\right) \\ &= \begin{bmatrix}1\\ 1\end{bmatrix} a\exp(i\omega t)\left[\cos(\Delta\omega t) - \sin(\Delta\omega t)\right] \\ \overrightarrow{E_{PD4}} &= \frac{1}{2}\begin{bmatrix}1 & 1\\ 1 & 1\end{bmatrix}\left(\vec{E_L} + \vec{E_R}\right) \\ &= \begin{bmatrix}1\\ 1\end{bmatrix} a\exp(i\omega t)\left[\cos(\Delta\omega t) + \sin(\Delta\omega t)\right] \end{aligned} \tag{5}$$

From Equations (3) and (5), the obtained intensity of PD1 can be derived as:

$$\begin{aligned} I_{PD1} &= \left|\overrightarrow{E_{PD1}}\right|^2 \\ &= 2a^2\left[1 + \cos\left(\frac{4\pi v}{d}t\right)\right] \\ &= 2a^2\left[1 + \cos\left(\frac{4\pi\Delta x}{d}\right)\right] \end{aligned} \tag{6}$$

Similarly, the intensity of the interferometric patterns on other PDs can be expressed as below:

$$\begin{aligned} I_{PD2} &= 2a^2\left[1 - \cos\left(\frac{4\pi\Delta x}{d}\right)\right] \\ I_{PD3} &= 2a^2\left[1 + \sin\left(\frac{4\pi\Delta x}{d}\right)\right] \\ I_{PD4} &= 2a^2\left[1 - \sin\left(\frac{4\pi\Delta x}{d}\right)\right] \end{aligned} \tag{7}$$

Four orthogonal intensity signals are then calculated to define the direction of the linear motion. To eliminate common-mode noise and to enhance the resolution by interpolation, we can remove the DC term as well as

Copyright © 2011 International Journal of Automation and Smart Technology

amplify the AC term of the intensity signal by a differential amplifier:

$$A = I_{PD1} - I_{PD2} = 4a^2 \cos\left(\frac{4\pi\Delta x}{d}\right)$$
$$B = I_{PD3} - I_{PD4} = 4a^2 \sin\left(\frac{4\pi\Delta x}{d}\right) \quad (8)$$

The two signals from Equation (8) form a Lissajous circle pattern. The relationship between the motion of the grating and the phase of the Lissajous circle is

$$\Delta x = \frac{d}{4\pi}\tan^{-1}\left(\frac{B}{A}\right) \quad (9)$$

Equation (9) implies that for the holographic gratings of 1200 lines/mm (0.833 µm in pitch), a Lissajous circle changes by 2π when the grating moves by 416.7 nm.

The above-mentioned encoding technique of LDGI forms the foundation of PDGI. A beam incident to the planar grating will diffract to four first-order diffracted beams in different directions (m=±1, n=0),(m=0, n=±1). Assuming the grid is perfectly aligned to the direction of movement, a specially designed optical configuration of combining two LDGIs, called PDGI, can encode these diffracted beams into the displacement of X-direction or Y-direction individually. PDGI is composed of two optical modules of LDGI in orthogonal configuration, as shown in Figure 3.

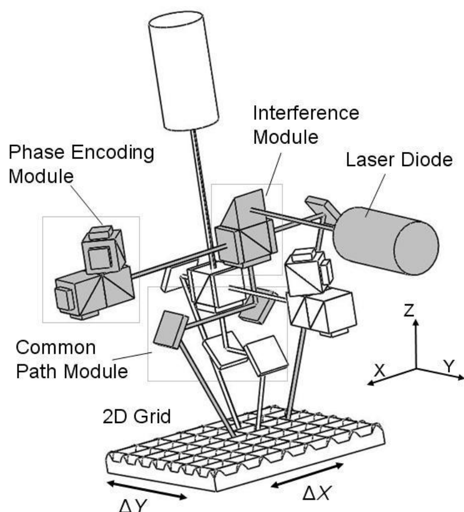

Figure 3. Optical configuration of PDGI.

Analysis of Alignment Tolerances

The head-to-scale alignment tolerances affect the performance of any grating interferometer. Figure 4 shows the motions of the planar grating. Two criteria are adopted to evaluate the head-to-scale alignment tolerances:

(1) The beam separation at PD must be less than the quarter diameter of the laser spots in order to maintain a sufficient fringe signal, as shown in Figure 5.

(2) The fringe must be located within the effective area of PD to prevent the signal loss, as shown in Figure 6.

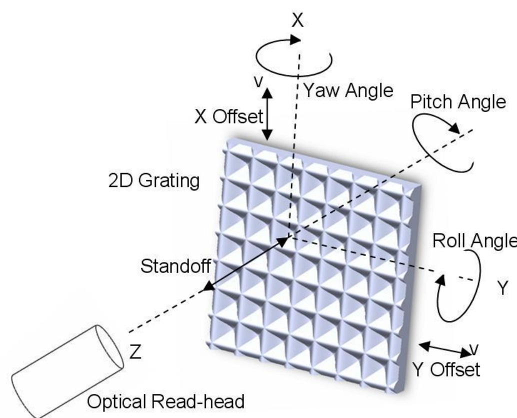

Figure 4. Motions of the planar grating.

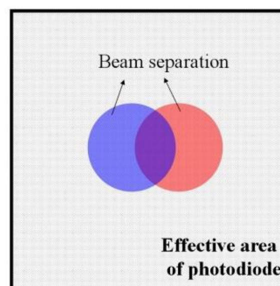

Figure 5. Beam separation.

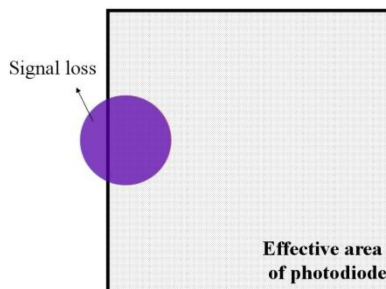

Figure 6. Signal loss from photodiode.

These geometrical tolerances can be quantitatively simulated by using a ray-tracing program [10]. The results of the alignment tolerances calculated by LightTools™ are listed in Table 2. It is evident that the alignment tolerances have very high tilt tolerances (Yaw, Roll) and distance tolerances (standoff) between the optical head and the grating which benefits from the Littrow configuration.

Copyright © 2011 International Journal of Automation and Smart Technology

Table 2. Allowable tolerance of the head to scale motion.

Motion of the planar grating	***Spots movement on PD***	***Values (unit)***
Yaw (θxz)		±1.15 (degree)
Roll (θyz)		±1.25 (degree)
Pitch (θxy)		±16 (arc min)
Standoff (Z-direction)		∞
Offset (X-direction)		±20 (mm)
Offset (Y-direction)		±20(mm)

Signal Processing

For the positioning measurement up to nanometer resolution, the signal waveform must be corrected to an ideal shape. In classical orthogonal waveforms there are three major error sources. As described by Heydemann [11], these are:

(1) lack of quadrature (ϕ)
(2) unequal gain in two channels ($a_1 \neq a_2$)
(3) DC drift (σ_1 and σ_2).

Therefore, defective signals occur in the forms of equations below:

$$\begin{aligned} A &= a_1 \sin(\theta + \phi) + \sigma_1 \\ B &= a_2 \cos\theta + \sigma_2 \end{aligned} \qquad (10)$$

A signal processing circuit is designed to correct these errors. To correct the first error, vector summation and subtraction is used in order to obtain the exact orthogonal waveforms. The latter two errors are corrected by sending the signal through a differential amplifier with appropriate magnification, while at the same time diminishing the common mode noise and DC drift. Figure 7 shows the diagram of a PDGI signal processing circuit.

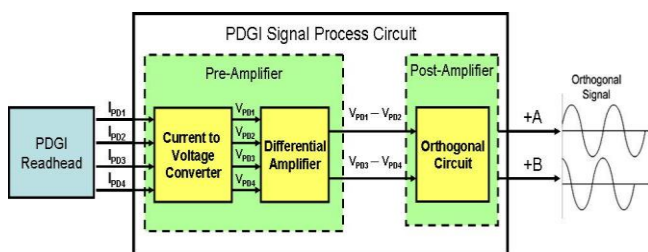

Figure 7. Diagram of PDGI signal process circuit.

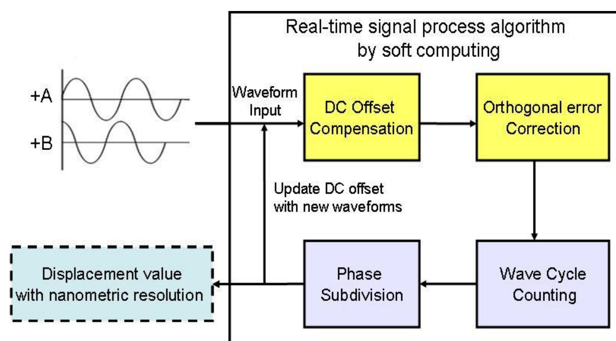

Figure 8. Diagram of real-time soft computing program.

Although the hardware based processor can provide faster processing, it cannot deal with complicated computation due to limited memory size. Therefore, a real-time signal processing by soft computing is also developed for this purpose. The block diagram of the soft computing is shown in Figure 8. The software is able to calculate dynamic waveform errors in real-time. Pulse counting and digital subdivision by arc-tangent function are also included in the software to achieve nanometric resolution. The pulse counting can be employed directly with respect to the corrected waveforms by software without the necessity of square wave transformation. Real-time signal processing algorithms carried out by soft computing makes the PDGI more robust and accurate when the geometrical errors of the moving stage occur.

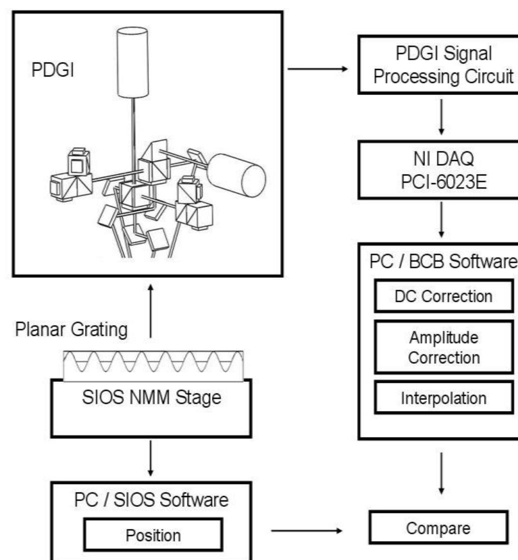

Figure 9. Experiment diagram of PDGI on SIOS stage.

Experiments and Results

Experiments were designed to test the performance of the PDGI system. Figure 9 shows the experimental layout. The 2D grid is carried by the XY stage of the Nanomeasuring Machine (NMM) of SIOS Co. The PDGI reads the interference intensity signals in two

Copyright © 2011 International Journal of Automation and Smart Technology

Figure 10. Photograph of PDGI.

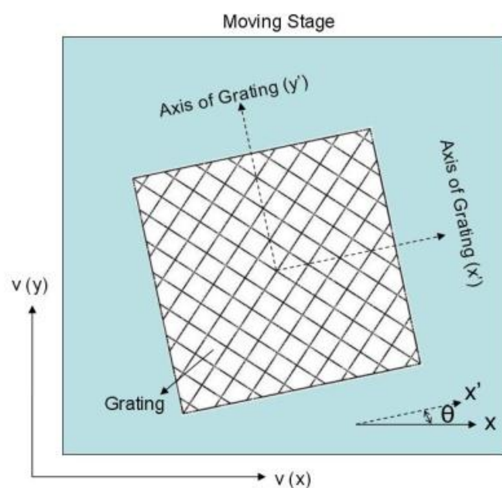

Figure 11. Misalignment between moving axes and measuring axes.

directions, which is converted into voltage signals through the processing circuit. The signals are sent to a PC via a NI PCI-6023 DAQ for soft computing, including error correction, up/down counting and waveform subdivision. The measured displacement value is then compared with the true displacement of the NMM, which is measured by laser interferometer. Figure 10 shows the photograph of an assembled PDGI. The physical size is only about 5 cm square.

The measurement errors of seven travels in the X-direction for positions from 0.1 to 25 mm are shown in Table 3. It can be seen that the measurement errors were dominated by the cosine error which is caused by inevitable misalignment between the moving coordinates (X-Y) and the grid coordinates (X'-Y'), as shown in Figure 11. Residual errors after least-squares line fitting show that the maximum positioning error is 17 nm and the standard deviations vary only from 3 to 15 nm.

The results of seven travels in the Y-direction for positions from 0.1 to 25 mm are shown in Table 4. After removing cosine error, the residual errors are within 20 nm and the standard deviations are from 3 to 11 nm only. These experimental results demonstrate the developed planar encoder to be a long range and highly repeatable 2D displacement sensor.

Table 3. Measurement error tests in X-axis.

Displacement (x)	*Measurement Error (Avg.) (nm)*	*Residual Error (nm)*	*Standard Deviation (nm)*
0-0.1 mm	2.9	5.7	2.9
0-1 mm	80	5.9	6.1
0-5 mm	420.8	8.9	7.9
0-10 mm	857.4	2.0	8.0
0-15 mm	1302.4	-13.4	8.1
0-20 mm	1720.1	-1.4	14.7
0-25 mm	2131.3	17.1	11.7

Table 4. Measurement error tests in Y-axis

Displacement (Y)	*Measurement Error (Avg.) (nm)*	*Residual Error (nm)*	*Standard Deviation (nm)*
0-0.1 mm	2	-6.6	3.1
0-1 mm	82.9	-3.4	7.5
0-5 mm	421.1	-10.6	9.3
0-10 mm	853.5	-9.9	9.4
0-15 mm	1313.4	18.3	8.0
0-20 mm	1729.4	2.6	11.4
0-25 mm	2138.9	-19.6	9.9

Summary

This paper presents a novel planar encoder system using grating interferometry. The system obtains 2-dimensional displacement information by using Doppler effect. Special optical configuration simplifies the whole structure and also enhances the alignment tolerance. Application of polarization theory optimizes the intensity of the orthogonal signals and the resolution of displacement value. The whole optical read head is minimized to 40×40×45 mm^3 which is considerably compact. A process circuit effectively decreases the main errors of two sinusoidal signals. Also, soft computing was developed to compute real-time signal compensation and subdivision. The results demonstrate the measurement errors in both directions are better than 20 nm for a 25 mm long travel in a normal laboratory environment.

Copyright © 2011 International Journal of Automation and Smart Technology

References

[1] C. F. Kao, S. H. Lu, H. M. Shen, and K. C. Fan, "Diffractive laser encoder with a grating in littrow configuration," *Japanese Journal of Applied Physics,* vol. 47, pp. 1833-1837, 2008.
doi: 10.1143/JJAP.47.1833

[2] K. C. Fan and Z. F. Lai, "An intelligent nano-positioning control system driven by an ultrasonic motor,," *International Journal of Precision Engineering and Manufacturing,* vol. 9, no. 3, pp. 40-45, 2008.

[3] K. C. Fan, Y. T. Fei, X. F. Yu, Y. J. Chen, W. L. Wang, F. Chen, and Y. S. Liu, "Development of a low-cost micro-cmm for 3d micro/nano measurements," *Measurement Science and Technology,* vol. 17, pp. 524-532, 2006.
doi: 10.1088/0957-0233/17/3/S12

[4] S. Ichikawa, M. Suzuki, W. Ishibashi, and S. Kuroki, "Two-dimensional optical encoder with three gratings in each dimension " US Patent 5204524, 1993.

[5] C. K. Lee, C. F. Kao, and C. C. Chang, "Conjugate optical path of a two-dimensional displacement measurement method," Taiwan Patent 153885, 2002.

[6] W. Gao, S. Dejima, and S. Kiyono, "A dual-mode surface encoder for position measurement," *Sensors and Actuators A: Physical,* vol. 117, no. 1, pp. 95-102, 2005.
doiI: 10.1016/j.sna.2004.06.004

[7] C. F. Kao, C. C. Chang, and C. F. Lin, "Apparatus for detecting displacement of two-dimensional motion," Taiwan Patent I224351, 2005.

[8] W. Gao and A. Kimura, "A three-axis displacement sensor with nanometric resolution," *CIRP Annals - Manufacturing Technology,* vol. 56, no. 1, pp. 529-532, 2007.
doi: 10.1016/j.cirp.2007.05.126

[9] A. Kimura, W. Gao, Y. Arai, and Z. Lijiang, "Design and construction of a two-degree-of-freedom linear encoder for nanometric measurement of stage position and straightness," *Precision Engineering,* vol. 34, no. 1, pp. 145-155, 2010.
doi: 10.1016/j.precisioneng.2009.05.008

[10] *Lighttools user's guide*. Pasadena, CA: Optical Research Associates, 2000.

[11] P. L. M. Heydemann, "Determination and correction of quadrature fringe measurement errors in interferometers," *Applied Optics,* vol. 20, no. 19, pp. 3382-3384, 1981.
doi: 10.1364/AO.20.003382

Copyright © 2011 International Journal of Automation and Smart Technology